Submitted to the Annals of Applied Statistics

STATISTICAL ANALYSIS OF A DYNAMIC MODEL FOR DIETARY CONTAMINANT EXPOSURE

By Patrice Bertail*, Stéphan Clémençon and Jessica Tressou†

Université Paris X, Telecom ParisTech and INRA-Mét@risk

This paper is devoted to the statistical analysis of a stochastic model introduced in Bertail, Clémençon & Tressou (2007) for describing the phenomenon of exposure to a certain food contaminant. In this modeling, the temporal evolution of the contamination exposure is entirely determined by the accumulation phenomenon due to successive dietary intakes and the pharmacokinetics governing the elimination process in between intakes, in such a way that the exposure dynamic through time is described as a *piecewise deterministic Markov process*. Paths of the contamination exposure process are scarcely observable in practice, therefore intensive computer simulation methods are crucial for estimating the time-dependent or steady-state features of the process. Here we consider simulation estimators based on consumption and contamination data and investigate how to construct accurate bootstrap confidence intervals for certain quantities of considerable importance from the epidemiology viewpoint. Special attention is also paid to the problem of computing the probability of certain rare events related to the exposure process path arising in dietary risk analysis using multilevel splitting or importance sampling techniques. Applications of these statistical methods to a collection of datasets related to dietary methyl mercury (MeHg) contamination are discussed thoroughly.

1. Introduction. Food safety is now receiving increasing attention both in the public health community and in scientific literature. For example, it was the second thematic priority of the 7th European Research Framework Program (refer to http://ec.europa.eu/research/fp7/) and advances in this field are starting to be reported in international conferences, as attested by the session *statistics in environmental and food sciences* in the 25th European Meeting of Statisticians held in Oslo in 2005, or in the *38èmes journées de Statistique* held in Clamart, France, in 2006. Addition-

*The first author is also affiliated to CREST-LS, Malakoff, France.

†The third author is a visiting scholar at the Hong Kong University of Science and Technology, her research is partly supported by Hong Kong RGC Grant #601906.

AMS 2000 subject classifications: Primary 92D30; secondary 62D05, 62E20

Keywords and phrases: food safety risk analysis, dietary contamination, linear pharmacokinetics model, piecewise deterministic Markov process, long run behavior, Monte-Carlo techniques, simulation estimator, bootstrap, rare event analysis

ally, several pluridisciplinary research units dedicated entirely to dietary risk analysis, such as Met@risk (INRA, http://metarisk.inapg.inra.fr) in France, Biometris (www.biometris.nl) in the Netherlands or the Joint Institute for Food Safety and Applied Nutrition in the United States (www.foodrisk.org) have recently been created. This rapidly developing field involves various disciplines across the medical, biological, social and mathematical sciences. The role of Statistics in this field is becoming more and more widely recognized; see the seminal discussion in [32], and consists particularly of developing probabilistic methods for quantitative risk assessment, refer to [5; 14; 20; 41]. Hence, information related to the contamination levels of an increasing number of food products for a wide range of chemicals on the one hand and to the dietary behavior of large population samples on the other hand is progressively collected in massive databases. The study of dietary exposure to food contaminants has raised many stimulating questions and motivated the use and/or development of appropriate statistical methods for analyzing the data, see [4; 37] for instance. Recent work focuses on static approaches for modeling the quantity X of a specific food contaminant ingested over a short period of time and computing the probability that X exceeds a maximum tolerable dose, eventually causing adverse effects on human health; see [36] and the references therein. One may refer to [3; 32] for a detailed account of dose level thresholds such as the *Provisional Tolerable Weekly Intake*, meant to represent the maximum contaminant dose one may ingest per week without significant risk. However, as emphasized in [2], it is essential for successful modeling to take account of the human kinetics of the chemical of interest when considering contaminants such as methyl mercury (MeHg), our running example in this paper, that is not eliminated quickly, with a biological *half-life* measured in weeks rather than days, as detailed in section 2. In [2], a dynamic stochastic model for dietary contamination exposure has been proposed, which is driven by two key components: the accumulation phenomenon through successive dietary intakes and the kinetics in man of the contaminant of interest that governs the elimination process. While a detailed study of the structural properties of the exposure process, such as communication and stochastic stability, has been carried out in [2], the aim of the present paper is to investigate the relation of the model to available data so as to propose suitable statistical methods.

The rest of the article is organized as follows. In section 2, the dynamic model proposed in [2] and its structural properties are briefly reviewed, with the aim of giving an insight into how it is ruled by a few key components. In section 3, the relation of the dynamic exposure model previously described to available data is thoroughly investigated. In particular, we show

how computationally-intensive methods permit the analysis the data in a valid asymptotic theoretical framework. Special emphasis is placed on the problem of bootstrap confidence interval construction from simulation estimates of certain features of the exposure process, which are relevant from the epidemiology viewpoint. Statistical estimation of the probability of certain rare events, such as those related to the time required for the exposure process to exceed some high and potentially critical contamination level, for which naive Monte-Carlo methods obviously fail, is also considered. *Multilevel splitting* genetic algorithms or *importance sampling* techniques are adapted to tackle this crucially important issue in the field of dietary risk assessment. This is followed by a section devoted to the application of the latter methodologies for analyzing a collection of datasets related to dietary MeHg contamination, in which the eventual use of the model for prediction and disease control from a public health guidance perspective is also discussed. Technicalities are deferred to the Appendix.

2. Stochastic Modeling of Dietary Contaminant Exposure. In [2] an attempt was made to model the temporal evolution of the total body burden of a certain chemical present in a variety of foods involved in the diet, when contamination sources other than dietary, such as environmental contamination for instance, are neglected. As recalled below, the dynamic of the general model proposed is governed by two key components, a marked point process (MPP) and a linear differential equation, in order to appropriately account for the accumulation of the chemical in the human body and its physiological elimination respectively.

Dietary behavior. The accumulation phenomenon of the food contaminant in the body occurs according to the successive dietary intakes, which may be mathematically described by a marked point process. Assume that the chemical is present in a collection of P types of food, indexed by $p = 1, \cdots, P$. A meal is then modeled as a random vector $Q = (Q^{(1)}, \cdots, Q^{(P)})$, the p-th component $Q^{(p)}$ indicating the quantity of food of type p consumed during the meal, with $1 \leq p \leq P$. Suppose that also, for $1 \leq p \leq P$, food type p eaten during a meal is contaminated in random ratio $C^{(p)}$ in regards to the chemical of interest. For this meal the total contaminant intake is then

$$U = \sum_{p=1}^{P} C^{(p)} Q^{(p)} = \langle C, Q \rangle, \tag{1}$$

of which distribution F_U is the image of the joint distribution $F_Q \otimes F_C$ by the standard inner product $\langle ., . \rangle$ on $\mathbb{R}^P$, denoting by F_Q the distribution

of the consumption vector Q and by F_C that of the contamination vector $C = (C^{(1)}, \cdots, C^{(P)})$, as soon as the r.v.'s Q and C are assumed to be independent of each other. Equipped with this notation, a stochastic process model that carries information about the times of the successive dietary intakes of an individual of the population of interest and the quantities of contaminant ingested, at the same time, may be naturally constructed by considering the marked point process $\{(T_n, Q_n, C_n)\}_{n\in\mathbb{N}}$, where the T_n's denote the successive times when a food of type $p \in \{1, \cdots, P\}$ is consumed by the individual and the second and third components of the MPP, Q_n and C_n, are respectively the consumption vector and the contamination vector related to the meal eaten at time T_n. One may naturally suppose that the sequence of quantities consumed $(Q_n)_{n\in\mathbb{N}}$ is independent from the sequence $(C_n)_{n\in\mathbb{N}}$ of chemical concentrations.

A given dietary behavior may now be characterized by stipulating specific dependence relations for the (T_n, Q_n)'s. When the chemical of interest is present in several types of food of which consumption is typically alternated or combined for reasons related to taste or nutritional aspects, assuming an autoregressive structure for the $(\Delta T_n, Q_n)$'s, with $\Delta T_n = T_n - T_{n-1}$ for all $n \geq 1$, seems appropriate. In addition, different portions of the same food may be consumed on more than one occasion, which suggests that, for a given food type p, assuming dependency among their contamination levels $C_n^{(p)}$'s may also be pertinent in some cases. However, in many important situations, it is reasonable to consider a very simple model in which the marks $\{(Q_n, C_n)\}_{n\in\mathbb{N}}$ form an i.i.d. sequence independent from the point process $(T_n)_{n\in\mathbb{N}}$, the latter being a pure renewal process, *i.e.* durations ΔT_n in between intakes are i.i.d. random variables. This modeling is particularly pertinent for chemicals largely present in one type of food. Examples include methyl mercury quasi-solely found in seafood products, certain mycotoxins such as Patulin exclusively present in apple products, see §3.3.2 in [16], or Chloropropanols, see §5.1 in [17]. Beyond its relevancy for such crucial cases in practice, though simple, this framework raises very challenging probabilistic and statistical questions, as shown in [2]. So that the theoretical results proved in this latter paper may be used for establishing a valid asymptotic framework, we also set ourselves under this set of assumptions in the present statistical study and leave for further investigation the issue of modeling more complex situations. Hence, throughout the article the accumulation of a chemical in the body through time is described thoroughly by the MPP $\{(T_n, U_n)\}_{n\in\mathbb{N}}$ with i.i.d. marks $U_n = \langle Q_n, C_n \rangle$ drawn from $F_U(dx) = f_U(x)dx$, the common (absolutely continuous) distribution of the intakes, independent from the renewal process $(T_n)_{n\in\mathbb{N}}$. Let $G(dt) = g(t)dt$

denote the common distribution of the inter-intake durations ΔT_n, $n \in \mathbb{N}$. Then, taking by convention $T_0 = 0$ for the first intake time, the total quantity of chemical ingested by the individual up to time $t \geq 0$ is

$$B(t) = \sum_{k=1}^{N(t)} U_k, \tag{2}$$

where $N(t) = \sum_{k\in\mathbb{N}} \mathbb{I}_{\{T_k \leq t\}}$ is the number of contaminant intakes up to time t, denoting by $\mathbb{I}_{\mathcal{A}}$ the indicator function of any event $\mathcal{A}$.

Pharmacokinetics. Given the metabolic rate of a given organism, physiological elimination/excretion of the chemical in between intakes is classically described by an ordinary differential equation (ODE), the whole human body being viewed as a *single compartment pharmacokinetic model*, see [19; 33] for an account of pharmacokinetic models. Supported by considerable empirical evidence, one may reasonably assume the elimination rate to be proportional to the total body burden of the chemical in numerous situations, including the case of methyl mercury:

$$dx(t) = -\theta x(t) \cdot dt, \tag{3}$$

denoting by $x(t)$ the total body burden of chemical at time t. The acceleration parameter $\theta > 0$ describes the metabolism with respect to the chemical elimination. However in pharmacology/toxicology, the elimination rate is classically measured by the *biological half-life* of the chemical in the body, $\log(2)/\theta$, that is the time required for the total body burden x to decrease by half in the absence of a new intake. One may refer to [6] for basics on linear pharmacokinetics systems theory, pharmacokinetics parameters, and standard methodologies for designing experiments and inferring numerical values for such parameters.

Remark 1. Modelling variability in the metabolic rate *In order to account for variability in the metabolic rate while preserving monotonicity of the solution $x(t)$, various extensions of the model above may be considered. A natural way consists of incorporating a 'biological noise' and randomizing the ODE (3), replacing θdt by $d\mathcal{N}(t)$, where $\{\mathcal{N}(t)\}_{t\geq 0}$ denotes a time-homogeneous (increasing) Poisson process with intensity θ (and compensator θt):*

$$dx(t) = -x(t) \cdot d\mathcal{N}(t).$$

The results recalled below may be easily extended to this more general framework. However, as raw data related to physiological elimination of dietary

contaminants are very seldom in practice, this prevents us from fitting a sophisticated model in a reliable fashion, therefore we restrict ourselves to the simple model described by Eq. (3) on the grounds of parsimony.

Let $X(t)$ denote the total body burden of a given chemical at time $t \geq 0$. Under the assumptions listed above, the *exposure process* $X = \{X(t)\}_{t\geq 0}$ moves deterministically according to the first order differential equation (3) in between intakes and has the same jumps as $(B(t))_{t\geq 0}$. A typical càd-làg[1] sample path of the exposure process is displayed below in Figure 1. Let $A(t) = t - T_{N(t)}$ denote the *backward recurrence time* at $t \geq 0$ (*i.e.* the time since the last intake at t). The process $\{(X(t), A(t))\}_{t\geq 0}$ belongs to the class of so-termed *piecewise deterministic Markov* (PDM) processes. Since the seminal contribution of [12], such stochastic processes are widely used in a large variety of applications in operations research, ranging from queuing systems to storage models. Refer to [13] for an excellent account of PDM processes and their applications. In most cases, the ΔT_n's are assumed to be exponentially distributed, making X itself a Markov process and its study much easier to carry out, see Chapter XIV in [1]. However, this assumption is clearly inappropriate in the dietary context and PDM models with increasing hazard rates are more realistic.

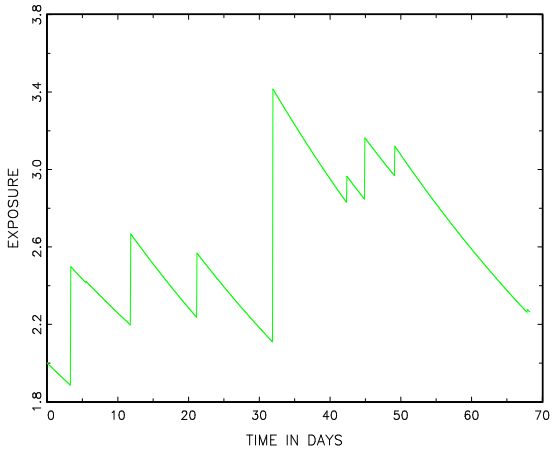

FIG 1. *Sample path of the exposure process* $X(t)$.

In [2], the structural properties of the exposure process X have been thoroughly investigated using an embedded Markov chain analysis, namely

[1]Recall that a mapping $x :]0, \infty[\to \mathbb{R}$ is said to be *càd-làg* if for all $t > 0$, $\lim_{s\to t,\ s>t} x(s) = x(t)$ and $\lim_{s\to t,\ s<t} x(s) = x(t-) < \infty$

by studying the behavior of the chain $\tilde{X} = (X_n)_{n\in\mathbb{N}}$ describing the exposure process immediately after each intake: $X_n = X(T_n)$ for all $n \in \mathbb{N}$. As a matter of fact, the analysis of such a chain is facilitated considerably by its autoregressive structure:

$$\left\{ \begin{array}{rcl} X_{n+1} & = & X_n e^{-\theta\Delta T_{n+1}} + U_{n+1},\ n \in \mathbb{N} \\ X_0 & = & x_0. \end{array} \right. \tag{4}$$

Such autoregressive models with random coefficients have been widely studied in the literature, refer to [30] for a recent survey of available results on this topic. The continuous-time process X may be easily related to the embedded chain $\tilde{X}$: solving (3) gives for all $t \geq 0$

$$X(t) = X_{T_{N(t)}} e^{-\theta A(t)}. \tag{5}$$

Long-term behavior. Under the conditions listed below, the behavior of the exposure process X in the long run can be determined.

(i) The inter-intake time distribution G has an infinite tail and either $\inf_{x\in]0,\epsilon]} g(x) > 0$ for some $\epsilon > 0$ or the intake distribution F_U has infinite tail.
(ii) There exists some $\gamma \geq 1$ such that $\mathbb{E}[U_1^\gamma] < \infty$.
(iii) The inter-intake time distribution has first and second order finite moments $m_G = \mathbb{E}[\Delta T_1] < \infty$ and $\sigma_G^2 = var[\Delta T_1] < \infty$.
(iv) There exists some $\delta > 0$ such that $\mathbb{E}[e^{-\delta\Delta T_1}] < \infty$.

These mild hypotheses can easily be checked in practice as we do in section 4 for MeHg: assumption (i) stipulates that inter-intake times may be arbitrarily long with positive probability and they may also either be arbitrarily short with positive probability, which may then also satisfy the exponential moment condition (iv), or intakes may otherwise be arbitrarily large with positive probability, but also 'relatively small' in the case when (ii) is fulfilled. In the detailed ergodicity study carried out in [2], Theorems 2 and 3 establish in particular that under conditions (i)-(iv), respectively conditions (i)-(ii), the continuous-time exposure process $X(t)$, respectively the embedded chain X_n corresponding to successive exposure levels at intake times, settles to an *equilibrium/steady state* as $t \to \infty$, respectively as $n \to \infty$), described by a governing, absolutely continuous, probability distribution $\mu(dx) = f(x)dx$, respectively $\tilde{\mu}(dx) = \tilde{f}(x)dx$ for the embedded discrete chain. The limiting distributions μ and $\tilde{\mu}$ are related to one another by the following equation, see (15) in [2]:

$$\mu([u,\infty[) = m_G^{-1} \int_{x=u}^{\infty} \int_{t=0}^{\infty} t \wedge \frac{\log(x/u)}{\theta} \tilde{\mu}(dx) G(dt). \tag{6}$$

These stationary distributions are of vital interest to quantify steady-state or long term quantities, pertinent to the epidemiology viewpoint, such as

- the steady-state mean exposure

$$m_\mu = \int_{x=0}^{\infty} x\mu(dx) = \lim_{t\to\infty} \mathbb{E}[X(t) \mid X(0) = x_0], \text{ for any } x_0 \geq 0, \tag{7}$$

- the limiting average time the exposure process spent above some (possibly critical) threshold value $u > 0$,

$$\mu([u, \infty[) = \lim_{T\to\infty} \frac{1}{T} \int_{t=0}^{T} \mathbb{I}_{\{X(t)\geq u\}} dt. \tag{8}$$

In [2], a simulation study was carried out to evaluate the time to steady-state for women of chilbearing age in the situation of dietary MeHg exposure, that is the time needed for the exposure process to behave in a stationary fashion, which is also termed *burn-in* period in the MCMC method context. It was empirically shown that after 5 to 6 half lives, or about 30 weeks, the values taken by the exposure process can be considered as drawn from the stationary distribution, which is a reasonable horizon on the human scale.

3. Statistical Inference via Computer Simulation. We now investigate the relation of the exposure model described in section 2 to existing data. In the first place, it should be noticed that information related to the contamination exposure process is scarcely available at the individual level. It seems pointless to try to collect data for reconstructing individual trajectories: an experimental design measuring the contamination levels of all food ingested by a given individual over a long period of time would not actually be feasible. Inference procedures are instead based on data for the contamination ratio related to any given food and chemical stored in massive data repositories, as well as collected survey data reporting the dietary behavior of large samples over short periods of time. In the following, we show how computer-based methods may be used practically for statistical inference of the exposure process $X(t)$ from this kind of data. A valid asymptotic framework for these procedures is also established from the *stability analysis* of the probabilistic model carried out in [2].

3.1. *Naive Simulation Estimators.* Suppose we are in the situation described above and have at our disposal three sets of i.i.d. data $\mathbf{G}$, $\mathbf{C}$ and $\mathbf{Q}$ drawn from G, F_C and F_Q respectively, as well as noisy half-life data $\mathbf{H}$ such as those described in [18]. From these data samples, various estimation procedures may be used for producing estimators $\hat{\theta}$, $\hat{G}$ and $\hat{F}_U$ of θ, G and F_U,

also fulfilling conditions (i)-(iv), see Remark 6 in the Appendix. One may refer in particular to [4] for an account of the problem of estimating the intake distribution F_U from contamination and consumption data sets $\mathbf{C}$ and $\mathbf{Q}$, see also section 4 below. Although the law of the exposure process $X(t)$ given the initial value $X(0) = x_0$, which is assumed to be fixed throughout this section, is entirely determined by the pharmacokinetic parameter θ and the distributions G and F_U, quantities related to the behavior that are of interest from the toxicology viewpoint are generally very complex functionals $T(\theta, G, F_U)$ of these parameters, refuting the possibility of computing plug-in estimates $T(\hat{\theta}, \hat{G}, \hat{F}_U)$ explicitly. Apart from the mean-value (7) and the mean-time spent over some threshold value (8) in steady-state, among relevant quantities one may also consider for instance:

- the mean-time required for exceeding a threshold level $u > 0$, given by

$$ET_u = \mathbb{E}_{x_0}[\tau_u(X)] \text{ with } \tau_u(X) = \inf\{t \geq 0 : \ X(t) > u\}, \tag{9}$$

  denoting by $\mathbb{E}_{x_0}[.]$ the conditional expectation given $X(0) = x_0$, given by
- the expected maximum exposure value over a period of time [0,T]

$$EM_T = \mathbb{E}_{x_0}[\sup_{t\in[0,T]} X(t)], \tag{10}$$

- the *expected overshoot* above a level $u > 0$ in steady-state

$$EO_u = \mathbb{E}_\mu[X - u \mid X > u] = \int_{x=0}^{\infty} x f(u+x)dx/\mu(]u, \infty[), \tag{11}$$

  denoting by $\mathbb{E}_\mu[.]$ the expectation in steady-state.

Based on the estimate $\hat{\theta}$ and the probability distributions $\hat{G}$, $\hat{F}_U$ at our disposal, we are then able to simulate sample paths of the exposure process $\hat{X} = \{\hat{X}(t)\}_{t\geq 0}$ governed by these instrumental estimates. Although computing estimates of certain characteristics such as the ones mentioned above for $\hat{X}$ may be carried out straightforwardly via Monte-Carlo simulation, one should pay careful attention to whether a good approximation of (θ, G, F_U) also induces a good approximation of the corresponding characteristics of the exposure process, which is far from trivial. Considering the geometry of exposure trajectories shown in Figure 1, this may be viewed as a *stability/continuity* problem in the Skorohod space $\mathbb{D}_T$ of *càd-làg* functions $x : (0, T) \to \mathbb{R}$ equipped with an adequate topology (in a way that two exposure paths can possibly be 'close', although their respective jumps do not necessarily happen simultaneously) when $T < \infty$ (refer to [44] for

an excellent account of such topological path spaces). This issue has been handled in Theorem 5 of [2] using a coupling technique (see also Corollary 6 therein). Theorem 1 in the Appendix recapitulates these results from a statistical perspective and establishes the strong consistency of simulation estimators, provided that $\hat{\theta}$, $\hat{G}$ and $\hat{F}_U$ are strongly consistent estimates of θ, G and F_U as the sizes of the datasets **H**, **G**, **C** and **Q** become large.

In practice, one might be also interested in the behavior of such estimators as $T \to \infty$, with the aim of estimating steady-state features such as (7) or (8). The accuracy of simulation estimators not only depends on the closeness between (θ, G, F_U) and the instrumental parameters $(\hat{\theta}, \hat{G}, \hat{F}_U)$, but also on the runlength $T < \infty$ of the simulation. Indeed, a natural way for estimating the probability (8) that exposure exceeds some prescribed threshold u at equilibrium for instance is to compute a Monte-Carlo approximation of $\mathbb{E}[T^{-1}\int_{t=0}^{T}\mathbb{I}_{\{\hat{X}(t)\geq u\}}dt]$ for T adequately large. By virtue of Theorem 1 in the Appendix, for a fixed T, this is a consistent estimate of $\mathbb{E}[T^{-1}\int_{t=0}^{T}\mathbb{I}_{\{X(t)\geq u\}}dt]$, which converges in its turn to $\mu([u,\infty[)$ at an exponential rate when $T \to \infty$, see Theorem 3 in [2]. Theorem 2 in the Appendix shows that the inference method based on this heuristic is strongly consistent for estimating steady-state quantities such as (7), (8) or (11), provided that T grows to infinity at a suitable rate. Refer to §4.3 for numerical results in the MeHg exposure context.

3.2. *Bootstrap and Confidence Intervals.* Now that consistent inference procedures have been described in various important estimation settings, we naturally turn our attention to the problem of assessing statistical accuracy for the estimates thus computed. Given the technical difficulties faced when trying to identify asymptotic distributions of the simulation estimators described in §3.1, we take advantage of *bootstrap confidence intervals*, which are built directly from the data, via the implementation of a simplistic computer algorithm; see [22] for an account of the bootstrap theory, and [15] for a more practice-oriented overview. Here we discuss the application of the *bootstrap-percentile* method to our specific setting for automatically producing confidence intervals from simulation estimators.

Let us suppose that the parameter of interest is in the form of $F(\Phi) = \mathbb{E}[\Phi(X(t)\}_{t\in[0,T]})]$, where $T < \infty$ and $\Phi : \mathbb{D}_T \to \mathbb{R}$ is a given function defined in the exposure path space. As previously noted, typical choices are $x \mapsto \int_0^T \mathbb{I}_{\{x(t)\geq u\}}dt$ and $x \mapsto \int_0^T (x(t)-u)\mathbb{I}_{\{x(t)\geq u\}}dt$ for $u \geq 0$. We consider the problem of estimating the sampling distribution of a simulation estimator $\hat{F}(\Phi) = \mathbb{E}[\Phi(\{\hat{X}(t)\}_{t\in[0,T]})]$ of $F(\Phi)$ computed using instrumental parameter estimates $\hat{\theta}$, $\hat{G}$ and $\hat{F}_U$ fitted from data samples **H**, **G**, **C** and

Q: $\mathcal{F}_\Phi(x) = \mathbb{P}(\hat{F}(\Phi) - F(\Phi) \leq x)$. Note that here the probability refers to the randomness in the samples **H**, **G**, **C** and **Q**. The *'simulated bootstrap' algorithm* is performed in five steps as follows.

Algorithm 1 - 'Simulated Bootstrap'

1. Make i.i.d. draws with replacement in each of the four datasets **H**, **G**, **C** and **Q**, yielding the bootstrap samples $\mathbf{H}^*$, $\mathbf{G}^*$, $\mathbf{C}^*$ and $\mathbf{Q}^*$, with the same sizes as the original samples, respectively.
2. From data samples generated in step 1, compute bootstrap versions $\hat{\theta}^*$, $\hat{G}^*$ and $\hat{F}_U^*$ of the instrumental estimates $\hat{\theta}$, $\hat{G}$ and $\hat{F}_U$.
3. From the bootstrap parameters $\hat{\theta}^*$, $\hat{G}^*$ and $\hat{F}_U^*$, simulate the *bootstrap exposure process*: $\{\hat{X}^*(t)\}_{t\in[0,T]}$.
4. Compute the bootstrap estimate of the sampling distribution of $\hat{F}(\Phi)$

$$\mathcal{F}_\Phi^{BOOT}(x) = \mathbb{P}^*(\hat{F}^*(\Phi) - \hat{F}(\Phi) \leq x), \tag{12}$$

   where $\mathbb{P}^*$ denotes the conditional probability given the original datasets.
5. A bootstrap confidence interval at level $1-\alpha \in (1/2, 1)$ for the parameter $\hat{F}(\Phi)$ is obtained using the bootstrap root's quantiles $q^*_{\alpha/2}$ and $q^*_{1-\alpha/2}$, of orders $\alpha/2$ and $1-\alpha/2$ respectively:

$$\mathcal{I}^*_{1-\alpha} = [\hat{F}(\Phi) + q^*_{\alpha/2}, \hat{F}(\Phi) + q^*_{1-\alpha/2}]. \tag{13}$$

Here the redundant designation 'simulated bootstrap' simply emphasizes the fact that a path simulation stage follows the data resampling and parameter recomputing steps. Asymptotic validity of this bootstrap procedure may be established at length by refining the proof of Theorem 1, based on the Fréchet differentiability notion. Owing to space limitations, technicalities here are omitted.

Remark 2. Monte-Carlo approximations *The bootstrap distribution estimate (12) may be practically approximated by iterating B times the resampling step and averaging then over the B resulting bootstrap trajectory replicates: $\{\hat{X}^*_b(t)\}_{t\in[0,T]}$ with $b \in \{1, \ldots, B\}$.*

3.3. *Rare Event Analysis.* The statistical study of the extremal behavior of the exposure process is also of crucial importance in practice. Indeed, accurately estimating the probability of reaching a certain possibly critical level u within a lifetime is an essential concern from the public health perspective (see the discussion in section 4). When the toxicological threshold level u of interest is 'very high', when compared to the mean behavior of the

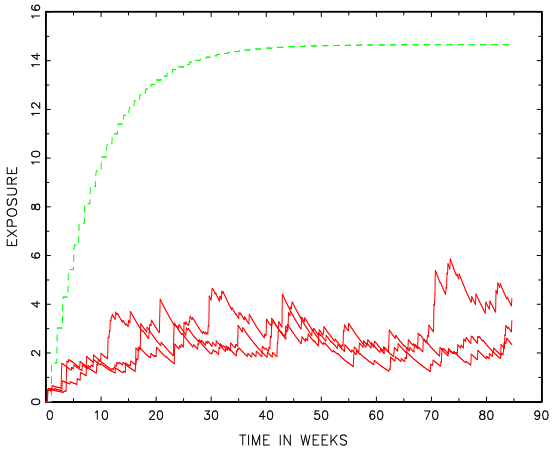

FIG 2. *Examples of trajectories in the French adult female population compared to a reference exposure process (Unit: µg/kg bw). The solid red curves are different trajectories with the same initial state $x_0 = 0$. The dashed green curve stabilizes at a critical threshold of reference u, see Section 4 for details on its construction.*

exposure process X, crude Monte-Carlo (CMC) methods, as those proposed in §3.1, completely fail; see Figure 3.3 for an illustration of this phenomenon. We are then faced with computational difficulties inherent to the issue of estimating the probability of a *rare event* related to X's law. In this paper, we leave aside the question of fully describing the extremal behavior of the exposure process X in an analytical fashion and infering values for related theoretical parameters such as the *extremal index*, measuring to what extent extreme values tend to come in 'small clusters'. Attention is rather focused on practical simulation-based procedures for estimating probabilities of rare events of the form $\mathcal{E}_{u,T} = \{\tau_u(X) \leq T\}$, where T is a reasonable horizon on the human scale, and level u is very large in comparison with the long term mean exposure m_μ for instance. Here, two methods are proposed for carrying out such a rare event analysis in our setting, each having its own advantages and drawbacks, see [21] for a review of available methods for estimating the entrance probability into a rare set. In the first approach, a classical *importance sampling* procedure is implemented, while our second strategy, based on an adequate factorization of the rare event probability $\mathbb{P}_{x_0}(\mathcal{E}_{u,T})$ relying on the Markov structure of the process $(X(t), A(t))$ (*i.e.* a Feynman-Kac representation), consists of using a *multilevel splitting* algorithm, see [9]. In the latter, simulated exposure trajectories getting close to the target level u are 'multiplied', while we let the others die, in the spirit of

the popular ReSTART (*Repetitive Simulated Trials After Reaching Thresholds*) method; refer to [43] for an overview. In section 4, both methodologies are applied in order to evaluate the risk related to dietary MeHg exposure, namely the probability that the total body burden rises above a specific dose of reference.

3.3.1. *Importance Sampling.* Importance sampling (*IS*) is a standard tool in rare event simulation. It relies on simulating exposure paths from a different probability, $\tilde{\mathbb{P}}$ say, equivalent to the original along a suitable filtration, chosen in a way that the event of interest $\mathcal{E}_{u,T}$ is much less rare, or even frequent, under the latter distribution, refer to [7] for a recent account of IS techniques and their applications. The rare event probability estimate is then computed by multiplying the empirical quantity output by the simulation algorithm using the new distribution by the corresponding likelihood ratio (*importance function*).

In our setting, a natural way of *speeding up* the exceedance of level u by process X is to consider an intake distribution $\tilde{F}_U(dx) = \tilde{f}_U(x)dx$ equivalent to F_U though much larger in the stochastic ordering sense (*i.e.* $\tilde{F}_U(x) << F_U(x)$ for all $x > 0$), so that large intakes may occur more frequently, and, simultaneously, an inter-intake time distribution $\tilde{G}(dt) = \tilde{g}(t)dt$ with same support as $G(dt)$ but stochastically much smaller (namely, $G(t) << \tilde{G}(t)$ for all $t > 0$), in order that the intake frequency is increased (see section 4 for specific choices in the MeHg case). In contrast, the elimination process cannot be slowed down, *i.e.* the biological half-life $\log 2/\theta$ cannot be increased, at the risk of no longer preserving equivalence between $\mathbb{P}$ and $\tilde{\mathbb{P}}$. To be more specific, let $\tilde{\mathbb{P}}_{x_0}$ be the probability measure on the same underlying measurable space as the one on which the original probability $\mathbb{P}_{x_0}$ has been defined, making X the process described in section 2. Under $\tilde{\mathbb{P}}_{x_0}$, the intakes $\{U_k\}_{k\geq 1}$, respectively the inter-intake times $\{\Delta T_k\}_{k\geq 1}$, are i.i.d. r.v.'s drawn from $\tilde{F}_U$, respectively from $\tilde{G}$, and $X_0 = x_0 \geq 0$. The distribution $\mathbb{P}_{x_0}$ is absolutely continuous with respect to the IS distribution $\tilde{\mathbb{P}}_{x_0}$ along the filtration $\mathcal{F}_t = \sigma((U_k, \Delta T_k);\ 1 \leq k \leq N(t)),\ t \geq 0$, that is the collection of σ-fields generated by the intakes and inter-intake times until time t. In addition, on $\mathcal{F}_T$, the likelihood ratio is given by

$$L_T = \frac{1 - G(T - T_{N(T)})}{1 - \tilde{G}(T - T_{N(T)})} \times \prod_{k=1}^{N(T)} \frac{f_U(U_k)}{\tilde{f}_U(U_k)} \cdot \frac{g(\Delta T_k)}{\tilde{g}(\Delta T_k)}. \tag{14}$$

Hence, denoting by $\tilde{\mathbb{E}}_{x_0}[.]$ the $\tilde{\mathbb{P}}_{x_0}$-expectation, we have the relationship

$$\mathbb{P}_{x_0}(\mathcal{E}_{u,T}) = \tilde{\mathbb{E}}_{x_0}[L_T \cdot \mathbb{I}_{\mathcal{E}_{u,T}}]. \tag{15}$$

From a practical angle, the expectation on the right hand side of (15) is estimated by simulating a large number of exposure trajectories of length T under the IS probability measure $\tilde{\mathbb{P}}_{x_0}$ and then applying a CMC approximation, which yields an unbiased estimate of the target $\mathbb{P}_{x_0}(\mathcal{E}_{u,T})$.

3.3.2. *Multilevel Splitting.* The approach described above involves specifying an appropriate change of measure (adequate df's $\tilde{F}_U$ and $\tilde{G}$), so as to simulate a random variable $L_T \cdot \mathbb{I}_{\mathcal{E}_{u,T}}$ with reduced variance under the new distribution $\tilde{\mathbb{P}}$, see Chapter 14 in [7]. Avoiding this delicate tuning step generally based on large-deviations techniques when tractable, the so-termed *multilevel splitting technique* has recently emerged as a serious competitor to the IS methodology, see [21]. This approach is indeed termed *non-intrusive*, insofar as it does not require any modification of the instrumental simulation distributions. Here, it boils down to represent the distribution of the exposure process exceeding the critical threshold u in terms of a Feynman-Kac *branching particle model*, see [29] for an account of Feynman-Kac formulae and their genealogical and interacting particle interpretations. Precisely, the interval $[0, u]$ in which the exposure process X evolves before crossing the level $x = u$ is split into sub-intervals corresponding to intermediary sublevels $0 < u_1 < \ldots < u_m < u$ the exposure path must pass before reaching the rare set $[u, \infty[$ and particles, in this case exposure paths, branch out as soon as they pass the next sublevel. Connections between such a physical approach of rare event simulation and approximations of Feynman-Kac distributions based on interacting particle systems are developed at length in [9]. We now recall the principle of the multilevel splitting algorithm used in section 4. Suppose that m intermediary sub-levels $0 < u_1 < \ldots < u_m < u_{m+1} = u$, are specified by the user (see Remark 3), as well as instrumental simulation parameters (F_U, G, θ) and $x_0 > 0$. Let $N \geq 1$ be fixed and denote the cardinal of any finite set $\mathcal{X}$ by $| \mathcal{X} |$. The algorithm is then performed in $m+1$ steps as follows.

Algorithm 2 - 'Multi-level Splitting'

1. Simulate N exposure paths from $x_0 < u_1$ of runlength T, indexed by $k \in \{1, \ldots, N\}$ and denoted by $X^{[k]} = \{X_t^{[k]}\}_{t \in [0,T]}$, $1 \leq k \leq N$.
2. For $j = 1, \ldots, m$:
   (a) Let $\mathcal{I}_{1,j}$ be the index subset corresponding to the exposure trajectories having reached level u_j before endtime T, *i.e.* such that $\tau_{u_j}^{[k]} = \inf\{t \geq 0;\ X_t^{[k]} \geq u_j\} < T$. Define $\mathcal{I}_{0,j}$ as the index subset corresponding to the other sample paths.

(b) For each path indexed by k' in $\mathcal{I}_{0,j}$, randomly draw k in $\mathcal{I}_{1,j}$ and redefine $X^{[k']}$ as the trajectory confounded with $X^{[k]}$ until time $\tau_{u_j}^{[k]}$, and prolongated until time T by simulation from the state $X^{[k]}(\tau_{u_j}^{[k]})$. Note that hitting times $\tau_{u_j}^{[k]}$ necessarily occur at intake times.

(c) Compute $P_j = \mid \mathcal{I}_{1,j} \mid /N$ and pass onto the next level u_{j+1}.

3. Output the estimate of the probability $\mathcal{P}_{x_0,u,T} = \mathbb{P}_{x_0}(\mathcal{E}_{u,T})$:

$$\hat{\mathcal{P}}_{x_0,u,T} = P_1 \times \ldots \times P_{m+1}, \tag{16}$$

where P_{m+1} is defined as the proportion of particles that have reached the final level u among those which have reached the previous sublevel u_m, that is $\mid \mathcal{I}_{1,m+1}|/N$.

Before illustrating how the procedure works on a toy example, below are two relevant remarks.

REMARK 3. ON PRACTICAL CHOICE OF THE TUNING PARAMETERS *Although a rigorous asymptotic validity framework has been established in [9] for* **Algorithm 2** *when the number N of particles gets arbitrarily large, the intermediary sublevels $u_1, \ldots, u_m$ must be selected by the user in practice. As noticed in [27], an optimal choice would consist of choosing the sublevels so that the probability to pass from $[u_j, \infty[$ to $[u_{j+1}, \infty[$ should be the same, whatever the sublevel j. Here we mention the fact that, in the numerical experiments carried out in section 4, the sublevels have been determined by using the adaptive variant of* **Algorithm 2** *proposed in [8], where the latter are picked in such a way that all probabilities involved in the factorization (16) are approximately of the same order of magnitude.*

REMARK 4. 'VALIDATION' *Stating the truth, estimating the probability of rare events such as $\mathcal{E}_{u,T}$ is a difficult task in practice and, when feasible, the numerical results provided by different possible methods should be compared for assessing the order of magnitude of the rare event probability of interest. It should also be mentioned that, in a very specific case, namely when F_U and G are both exponential distributions, the distribution of the hitting time τ_u may be explicitly computed through its Laplace transform using Dynkin's formula, see [26]. As an initial attempt, the latter may be thus used for computing a preliminary rough estimate of $\mathcal{P}_{x_0,u,T}$.*

A toy example. Figure 3 illustrates the way **Algorithm 2** works in the case of $N = 5$ trajectories starting from $x_0 = 3$ with $m = 2$ intermediary

levels ($u = (4, 5, 6)$) and a horizon T equal to one year in the model with exponential intake and inter-intake times distributions. Initially, all curves have reached the first intermediary level ($u = 4$) except the blue curve as shown in Figure 3(a). It is then restarted from the red curve at the exact point where it first reached $u = 4$ in Figure 3(b). Now, only the blue and black curves have reached the second intermediary level ($u = 5$). In Figure 3(c), all the other curves are thus restarted from one of these at the exact point where they first reached $u = 5$. Eventually, only the blue curve reached the level of interest $u = 6$. The probability of reaching 6 in less than one year is estimated by $4/5 \times 2/5 \times 1/5 = 6.4\%$.

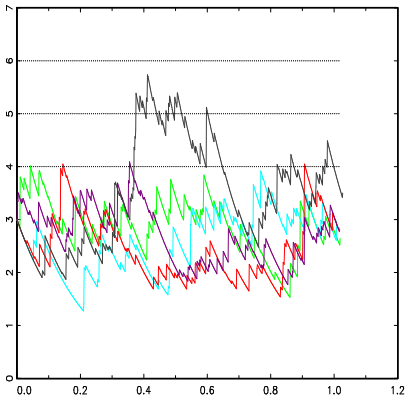

(a) Initialization: $N = 5$

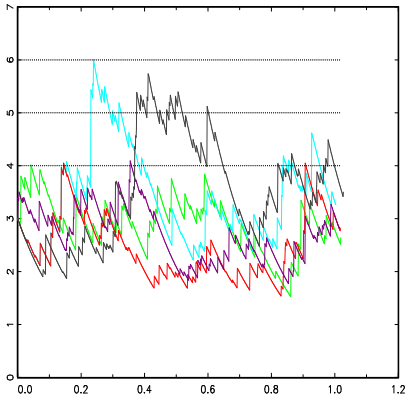

(b) Iteration 1: $u = 4$

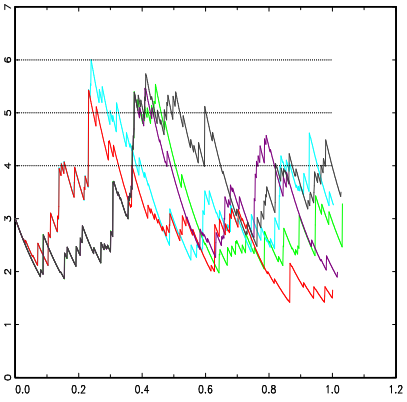

(c) Iteration 2: $u = 5$

FIG 3. *Multilevel Splitting: an illustration for $N = 5$ particles starting from $x_0 = 3$ with $m = 2$ intermediary levels ($u \in \{4, 5, 6\}$) and a horizon T equal to 1 year.*

4. Numerical results for MeHg exposure. In this section, we apply the statistical techniques presented in the preceding section for analyzing how women of childbearing age (who are female between 15 and 45, for the purpose of this study) are exposed to dietary MeHg, based on the dynamic model described in section 2. The group suffering the highest risk from this exposure is actually the unborn child as mentioned in the *hazard characterization step* described in [18]: the MeHg present in the seafood of the mother's diet will certainly pass onto the developing foetus and may cause irreversible brain damage.

From the available datasets related to MeHg contamination and fish consumption, essential features of the exposure process are inferred using the simulation-based estimation tools previously described. Special attention is now paid to the probability of exceeding a specific dose derived from a toxicological level of reference in the static setup, namely the *Provisional Tolerable Weekly Intake* (PTWI), which represents the contaminant dose an individual can ingest weekly over an entire lifetime without appreciable risk, as defined by the international expert committee of FAO/WHO, see [18]. This means it is crucial to implement the rare event analysis methods reviewed in §3.3.

Eventually, the impact of the choice of the statistical methods used for fitting the instrumental distributions is empirically quantified and discussed from the perspective of public health guidelines.

4.1. *Description of the datasets.* We start off with a brief description of the datasets used in the present quantitative risk assessment.

Contamination data C. Here we use the contamination data related to fish and other seafoods available on the French market that have been collected by accredited laboratories from official national surveys performed between 1994 and 2003 by the French Ministry of Agriculture and Fisheries [28] and the French Research Institute for Exploitation of the Sea [23]. This dataset comprises 2832 observations.

Consumption data G, Q. The national individual consumption survey INCA [10] provides the quantity consumed of an extensive list of foods over a week, among which fish and other seafoods, as well as the time consumption occurred with at least the information about the nature of the meal, whether it be breakfast, lunch, dinner or 'snacks'. It is surveys 1985 adults aged 15 years or over, including 639 adult females between 15 and 45. From these observations, the dataset **G** consists of the actual durations between consecutive intakes, when properly observed, together with right censored

inter-intake times, when only the information that the duration between successive intakes is larger than a certain time can be extracted from the observations. Inter-intake times are expressed in hours.

As in [2; 42], MeHg intakes are computed at each observed meal through a so-termed *deterministic procedure* currently used in national and international risk assessments. From the INCA food list, 92 different fish or seafood species are determined and a mean level of contamination is computed from the contamination data, as in [11; 38]. Intakes are then obtained through Eq. (1). For comparison sake, all consumptions are divided by the associated individual body weight, also provided in the INCA survey, so that intakes are expressed in migrograms per kilogram of body weight per meal ($\mu g/kgbw/meal$).

As previously mentioned, raw data related to the biological half-life of contaminants such as MeHg are scarcely available. Refering to the scientific literature devoted to the pharmacokinetics of MeHg in the human body (see [31; 34; 35; 25]), the biological half-life fluctuates at around 44 days. This numerical value, converted in hours, is thus retained for performing simulations, leading to pick $\log 2/(44 \times 24)$ for the acceleration parameter estimate $\hat{\theta}$.

4.2. *Estimation of the instrumental distributions F_U and G.* In order to estimate the cumulative distribution functions (cdf) of the intakes and inter-intake times, various statistical techniques have been considered, namely parametric and semi-parametric approaches.

Estimating the intake distribution. By generating intake data as explained in §4.1, we dispose of a sample $\mathbf{U}$ of $n_{F_U} = 1088$ intakes representative of the subpopulation consisting of women of childbearing age, on which the following cdf estimates are based.

Parametric modeling. We first considered two simple parametric models for the intake distribution: the first one stipulates that F_U takes the form of an exponential distribution with parameter $\lambda_{F_U} = 1/m_{F_U}$, while the other assumes it is a heavy-tailed Burr type distribution (with cdf $(1-(1+x^c)^{-k})$ for $c > 0$ and $k > 0$) in order to avoid underestimating the probability that very large intakes have occured. For both statistical models, related parameters have been set by the maximum likelihood estimation (*MLE*). It can be easily established that ML estimates are consistent and asymptotically normal in such regular models and, furthermore, that the cdf corresponding to the MLE parameter is also consistent in the L^1- sense, see Remark 6 in the Appendix. Numerically, based on $\mathbf{U}$ we found that $\hat{\lambda}_{F_U} = 4.06$ by simply inverting the sample mean in the exponential model, whereas in the Burr

distribution based model, MLE yields $\hat{c} = 0.95$ and $\hat{k} = 4.93$. Recall that, in the Burr case, $\mathbb{E}[U_1^\gamma] = \Gamma(k - \gamma/c) \times \Gamma(1 + \gamma/c)/\Gamma(k)$ is finite as soon as $ck > \gamma$. One may thus check that the intake distribution estimate fulfills condition (ii) with $\gamma = 4$; see section 2.

Semi-parametric approach. In order to allow for more flexibility and accuracy on the one hand and to obtain a resulting instrumental cdf well-suited for *worst case risk analysis* on the other hand, a semi-parametric estimator has also been fitted the following way: the piecewise linear left part of the cdf corresponds to a histogram-based density estimator, while the tail is modelled by a Pareto distribution, with a continuity constraint at the change point x_K. Precisely, a number k of extreme intakes is used to determine the tail parameter α of the Pareto cdf $1 - (\tau x)^{-\alpha}$, $\tau > 0$ and $\alpha > 0$, τ being chosen to ensure the continuity constraint. The value of k is fixed through a bias-variance trade-off, as in [38]. Numerically, we have $\alpha = 2.099$, $\tau = 5.92$, and $x_K = 0.355$.

Probability plots are displayed in Figure 4(a). The semi-parametric estimator clearly provides the best fit to the data. The Burr distribution is nevertheless a good parametric choice.

Estimating the inter-intake time distribution. We dispose of a sample $\mathbf{G}$ of $n_G = 1214$ right censored inter-intake times.

Parametric models. In this censored data setup, MLE boils down to maximizing the log likelihood given by

$$l(x, \delta, \nu) = \sum_{i=1}^{n_G} (1 - \delta_i) \log \left[f_\nu \left(x_i \right) \right] + \delta_i \ln \left[1 - F_\nu \left(x_i \right) \right],$$

where the (x_i, δ_i)'s are the observations, δ_i denotes the censorship indicator, f_ν is the density candidate, and F_ν the corresponding cdf. Four parametric distributions, widely used in survival analysis, have been considered here: Exponential, Gamma, Weibull and Log Normal. It is noteworthy that conditions (i)-(iv) listed in section 2 are satisfied for such distributions, except (iv) that is not fulfilled in the Log Normal case. One may also find that the cdf corresponding to the MLE parameter is L_1-strongly consistent for each of these regular statistical models. The resulting MLE estimators are: $\hat{\lambda}_G = 0.0078$ for the Exponential distribution $Exp(\lambda_G)$, $\hat{\alpha} = 1.06$ and $\hat{\beta} = 117.2$ for the Gamma distribution such that $1 - G(t) \propto t^{\alpha - 1} \exp(-t/\beta)$, $\hat{a} = 128.7$ and $\hat{c} = 0.999$ for the Weibull distribution such that $1 - G(t) = \exp(-(t/a)^c)$, and $\hat{a} = 4.41$ and $\hat{b} = 1.31$ for the Log Normal distribution, with parametrization such that $\log[(\Delta T_2 - a)/b)]$

follows a standard normal.

Semi-parametric modeling. Using a semi-parametric approach, a cdf estimate is built from a smoothed Kaplan-Meier estimator F_{KM} for the left part of the distribution and an exponential distribution for the tail behavior, with a continuity constraint at the change point. To be exact, the change point corresponds to the largest uncensored observation x_K and the parameter of the exponential distribution to $-\log[1 - F_{\mathrm{KM}}(x_K)]/x_K$, in a way that continuity at x_K is guaranteed. The resulting parameter of the exponential distribution is 0.0073, and $x_K = 146$ hours.

Figure 4(b) displays the corresponding probability plots. Again, the semi-parametric estimator provides the best fit, except naturally for the tail part because of the right censorship. The fitted Gamma distribution is marginally more accurate than the Weibull and Exponential distributions, since it offers the advantage of having an increasing hazard rate (here, $\alpha > 1$), which is a realistic feature in the dietary context.

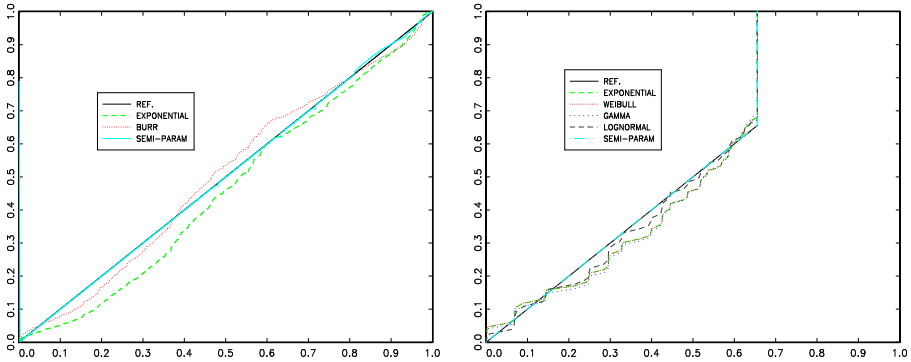

(a) F_U : Intake distribution (b) G : Inter-intake time distribution

FIG 4. *Probability plots, comparison of the different adjustments.*

4.3. *Estimation of the main features of the exposure process.* From the perspective of food safety, we now compute several important summary statistics related to the dietary MeHg exposure process of French females of childbearing age using the simulation estimators proposed in section 3. In chemical risk assessment, once a hazard has been identified, meaning that the potential adverse effects of the compound have been described, it is then characterized, using the notion of *threshold of toxicological concern*. This pragmatic approach for chemical risk assessment consists of specifying a threshold value, below which there is a very low probability of observing

TABLE 1
Estimation of the steady state mean and median for the 15 *models with* 95% *confidence intervals (unit:* $\mu g/kgbw$, $M = 1000$, $B = 200$*).*

	F_U : Exponential	F_U : Burr	F_U : Semi-Parametric
G :Exponential	$3.01 \in [2.68, 3.32]$	$2.96 \in [2.67, 3.23]$	$2.98 \in [2.67, 3.39]$
	$2.92 \in [2.53, 3.38]$	$2.97 \in [2.67, 3.24]$	$2.89 \in [2.53, 3.31]$
G :Gamma	$3.07 \in [2.69, 3.42]$	$3.03 \in [2.73, 3.34]$	$3.05 \in [2.69, 3.40]$
	$2.99 \in [2.57, 3.34]$	$3.04 \in [2.70, 3.31]$	$2.96 \in [2.57, 3.53]$
G :Weibull	$2.98 \in [2.63, 3.33]$	$2.97 \in [2.60, 3.29]$	$2.99 \in [2.67, 3.29]$
	$2.94 \in [2.54, 3.38]$	$2.96 \in [2.67, 3.23]$	$2.92 \in [2.47, 3.49]$
G :Log-Normal	$2.28 \in [2.02, 2.57]$	$2.25 \in [1.99, 2.54]$	$2.26 \in [1.95, 2.61]$
	$1.95 \in [1.63, 2.36]$	$2.45 \in [2.23, 2.70]$	$1.92 \in [1.56, 2.34]$
G : Semi-Parametric	$2.95 \in [2.67, 3.23]$	$2.90 \in [2.62, 3.25]$	$2.93 \in [2.58, 3.26]$
	$3.03 \in [2.71, 3.37]$	$2.83 \in [2.48, 3.16]$	$2.82 \in [2.42, 3.29]$

adverse effects on human health. In practice, one experimentally determines the lowest dose that may be ingested by animals or humans, daily or weekly, without appreciable effects. The *Tolerable Intake* is then established by multiplying this experimental value, known as the *Non Observed Adverse Effect Level* (NOAEL) by a relevant safety factor, taking into account both inter-species and inter-individual variabilities. This approach dates from the early sixties, see [39], and is internationally recognized in Food Safety, see [24]. The third and fourth steps of *risk assessment* consists of assessing the exposure to the chemical of interest for the studied population, and comparing it to the daily or weekly tolerable intake. The first two steps are known as *hazard identification* and *hazard characterization*, while the last two are called *exposure assessment* and *risk characterization*. In a static setup, when considering chemicals that are not accumulated in the human body and describing exposure by the supposedly i.i.d. sequence of intakes, this boils down to evaluating the probability that weekly intakes exceed the reference dose d, termed the *Provisionary Tolerable Weekly Intake* (PTWI), see [36]. Considering compounds with longer biological half-lives, we propose comparing the stochastic exposure process to the limit of a deterministic process of reference $\{x_n\}_{n\in\mathbb{N}}$. Mimicking the experiment carried out in the hazard characterization step, the latter is built up by considering intakes exactly equal to the PTWI d occuring every week (F_U is a point mass at d, and G is a point mass at one week, that is 7×24). The reference level is thus given by the affine recurrence relationship $x_n = \exp(-\log(2)/HL \times 1)x_{n-1} + d$, yielding a reference level $X_{\mathrm{ref},d} = \lim_{n\to\infty} x_n = d/(1 - 2^{-1/HL})$, where the half-life HL is expressed in weeks. For MeHg, the value $d = 0.7\ \mu g/kgbw/w$ corresponds to the reference dose established by the U.S. National Research

Council currently in use in the United States, see [40], whereas the PTWI has been set to $d = 1.6\ \mu g/kgbw/w$ by the international expert committee of FAO/WHO, see [18]. Numerically, this yields $X_{\text{ref},0.7} = 6.42\ \mu g/kgbw$ and $X_{\text{ref},1.6} = 14.67\ \mu g/kgbw$ when MeHg's biological half-life is fixed to $HL = 6$ weeks, as estimated in [35]. We termed this reference dose as 'Tolerable Body Burden' (TBB), which is more relevant than the previous 'Kinetic Tolerable Intake' (KTI) determined in [42].

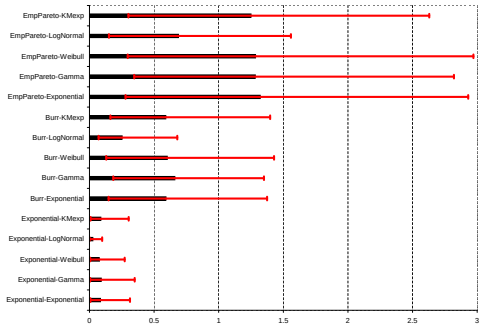

FIG 5. *Estimation of the steady state probability of exceeding* $u = 6.42$ *for the* 15 *models with* 95% *confidence intervals (unit: %,* $M = 1000$*,* $B = 200$*)*

In the dynamic setup, several summarizing quantities can be considered for comparison purposes. We first estimated two important features of the process of exposure to MeHg, for all combinations of input distributions: the long-term mean exposure m_μ, the median exposure value in the stationary regime, and the probability of exceeding the threshold $X_{\text{ref},0.7}$ in steady-state $\mu([X_{\text{ref},0.7}, \infty[)$; see Table 1 and Figure 5. Computation is conducted as follows: $M = 1000$ trajectories are simulated over a run length of 1 year after a *burn-in* period of 5 years, quantities of interest are then averaged over the M trajectories and this is repeated $B = 200$ times to build the bootstrap CI's, as described in section 3.2. The major differences among the 15 models for the stationary mean arise when using the Log Normal distribution for the inter-intake times with a lower estimation for this model presenting a heavy tail (longer inter-intake times are more frequent). All the other models for G lead to similar results in terms of confidence intervals for the mean and median exposures in the long run, whatever the choice for F_U, refer to Table 1. When estimating a tail feature such as the probability

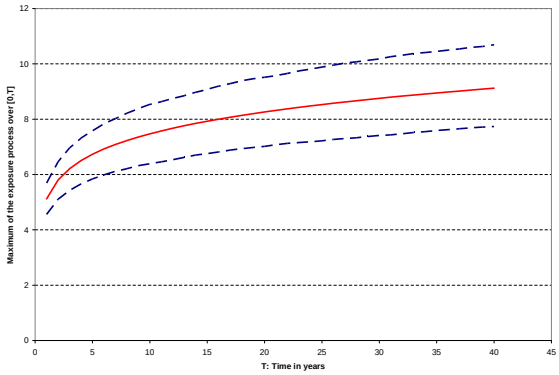

FIG 6. *Estimation of the expected maximum of the exposure process over* $[0, T]$ *as a function of the horizon* T *(*$M = 1000$*, and* $B = 200$*).*

of exceeding $u = X_{\text{ref},0.7}$ in steady-state, the choice of F_U becomes of prime importance, since its tail behavior is the same as that of the stationary distribution μ, see Theorem 3.2 in [2]. As illustrated by the notion of PTWI, risk management in food safety is generally treated in the framework of worst-case design. In the subsequent analysis, we thus focus on the Burr-Gamma model. Due to its 'conservative' characteristics, it is unlikely that it leads to an underestimation of the risk. It indeed stipulates heavy tail behavior for the intakes and light tail behavior for the inter-intake times.

Another interesting statistic is the expected overshoot over a safe level u. In the case of the 'Burr-Gamma' model and for $u = X_{\text{ref},0.7}$, the estimated expected overshoot is 0.101 $\mu g/kgbw$ with 95% bootstrap confidence interval $[0.033, 0.217]$, which corresponds to barely less than one average intake. Before turning to the case of level $u = X_{\text{ref},1.6}$, Figure 6 illustrates the fact that the exposure process very seldomly reaches such high thresholds displaying the estimation of the expected maximum over $[0, T]$ for different values of T.

Let us now turn to the main risk evaluation, that is, the estimation of the probability of reaching $u = X_{\text{ref},1.6} = 14.67$ within a reasonable time horizon. The application of the two methodologies described in section 3.3 are investigated for several time horizons, $T = 5, 10, 15$, and 20 years, in the Burr-Gamma model. Results are shown in Figure 7.

The application of the IS clearly illustrates the difficulty of choosing the right *IS* distribution. Indeed, in the present application, identifying the best Burr-Gamma model is not an easy task even though it is clear that one should select a Burr distribution stochastically greater than the original,

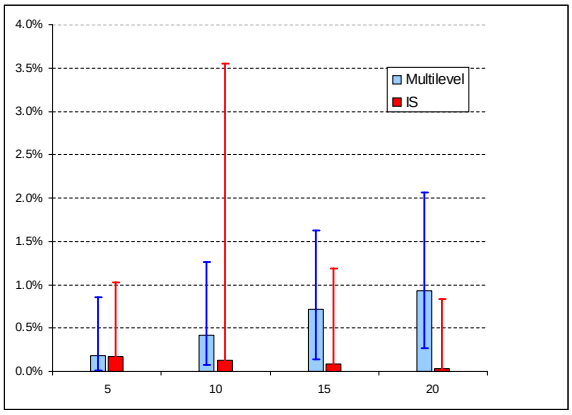

FIG 7. *Estimation of the probability of reaching* $u = X_{ref,1.6} = 14.67$ *within a reasonable time horizon (the importance distribution for IS is* $Burr(0.9, 4.5)$-$Gamma(1.01, 115)$*;* $M = 1000$ *is the size of the Monte carlo simulation used to approach the importance ratio, and* 95% *simulation intervals are computed over* $B = 100$ *iterations).*

and a Gamma distribution stochastically lower than the original one. For both distributions, we applied a mean translation to respectively increase the intakes and their frequency, as suggested in [7]. For example, if $T = 20$ years, if $\tilde{\mathbb{P}}_{x_0}$ is a Burr$(0.9, 4.5)$-Gamma$(1.01, 115)$ model, then only 63 trajectories out of $M = 1000$ exceed the threshold $u = X_{\text{ref},1.6} = 14.67$ so that $\mathbb{P}_{x_0}(\mathcal{E}_{u,T})$ is estimated at $2.91e-04$, with variance $4.40e-05$ (this is a median result over 100 iterations of the same simulation). Several other importance distributions were tested but the one presented here seems to be the more efficient in reducing the variance of the estimations, which are still quite large as shown in Figure 7.

We next consider the application of the Multilevel Splitting algorithm. A first simulation is conducted according to the adaptive multilevel algorithm proposed by [8] using $N = 1000$ particles to determine the intermediary levels $u_1, \ldots, u_m$ such that half the particles reach the next sublevel. For $T = 20$ years, the resulting levels are $7.85, 8.65, 9.47, 10.16, 11.07, 11.97$, and 13.08 for an estimated probability of 0.52%. Then running Algorithm 2 with these intermediary levels and $N = 500$ particles, we obtain an estimation of $\mathbb{P}_{x_0}(\mathcal{E}_{u,T})$ close to 1%. This result does not seem in coherence with our estimation of the maximum over $[0, T]$ with $T = 20$ years where the maximum reached over 1000 trajectories is much lower than 14.67 (less than 10) while it should be above 14.67 if this level has 1% chance to be reached. This suggests that additional work remains to be done in order to determine how to tune N as a function of T, when implementing this promising approach.

Nevertheless, for smaller time horizons T, Figure 7 shows that even though it certainly overestimates the rare event probability, the multilevel approach results in the probability of the rare event occurence increasing with the time horizon T contrary to IS.

References.

[1] Asmussen, S. (2003). *Applied Probability and Queues*. Springer-Verlag, New York.

[2] Bertail, P., Clémençon, S., and Tressou, J. (2008). A storage model with random release rate for modeling exposure to food contaminants. *Math. Biosc. Eng.* **35**, 1, 35–60.

[3] Bertail, P., Feinberg, M., Tressou, J., and (Coordinateurs), P. V. (2006). *Analyse des Risques Alimentaires*. TEC&DOC, Lavoisier, Paris.

[4] Bertail, P. and Tressou, J. (2006). Incomplete generalized U-Statistics for food risk assessment. *Biometrics* **62**, 1, 66–74.

[5] Boon, P., der Voet, H. V., and Klaveren, J. V. (2003). Validation of a probabilistic model of dietary exposure to selected pesticides in Dutch infants. *Food Addit. Contam.* **20**, Suppl. 1, S36–S39.

[6] Brett, M., Weimann, H., Cawello, W., Zimmermann, H., Pabst, G., Sierakowski, B., Giesche, R., and Baumann, A. (1999). *Parameters for Compartment-free Pharmacokinetics: Standardisation of Study Design, Data Analysis and Reporting*. Shaker Verlag, Aachen, Germany.

[7] Bucklew, J. (2004). *An Introduction to Rare Event Simulation*. Springer Series In Statistics. Springer.

[8] Cérou, F. and Guyader, A. (2007). Adaptative splitting for rare event analysis. *Stoch. Anal. Proc.* **25**, 2, 417–443.

[9] Cérou, F., Moral, P. D., LeGland, F., and Lezaud, P. (2006). Genetic genealogical models in rare event analysis. *Alea 1*, 183–196.

[10] CREDOC-AFSSA-DGAL. (1999). *Enquête INCA (individuelle et nationale sur les consommations alimentaires)*. TEC&DOC, Lavoisier, Paris. (Coordinateur : J.L. Volatier).

[11] Crépet, A., Tressou, J., Verger, P., and Leblanc, J. (2005). Management options to reduce exposure to methyl mercury through the consumption of fish and fishery products by the French population. *Regul. Toxicol. Pharmacol. 42*, 179–189.

[12] Davis, M. (1984). Piecewise-deterministic Markov processes: A general class of non-diffusion stochastic models. *J. R. Statist. Soc.* **46**, 3, 353–388.

[13] Davis, M. (1991). *Applied Stochastic Analysis*. Stochastics Monographs. Taylor & Francis.

[14] Edler, L., Poirier, K., Dourson, M., Kleiner, J., Mileson, B., Nordmann, H., Renwick, A., Slob, W., Walton, K., and Würtzen, G. (2002). Mathematical modelling and quantitative methods. *Food Chem. Toxicol. 40*, 283–326.

[15] Efron, B. and Tibshirani, R. J. (2004). *An Introduction to the Bootstrap*. Monographs on Statistics and Applied Probability. Chapman & Hall.

[16] FAO/WHO. (1995). Evaluation of certain food additives and contaminants. Forty-fourth report of the Joint FAO/WHO Expert Committee on Food Additives 859.

[17] FAO/WHO. (2002). Evaluation of certain food additives and contaminants. Fifty-seventh report of the Joint FAO/WHO Expert Committee on Food Additives 909.

[18] FAO/WHO. (2003). Evaluation of certain food additives and contaminants for methylmercury. Sixty first report of the Joint FAO/WHO Expert Committee on Food Additives, Technical Report Series, WHO, Geneva, Switzerland.

[19] Gibaldi, M. and Perrier, D. (1982). *Pharmacokinetics*. Drugs and the Pharmaceutical Sciences: a Series of Textbooks and Monographs. Marcel Dekker, New York. second edition.

[20] Gibney, M. and van der Voet, H. (2003). Introduction to the Monte Carlo project and the approach to the validation of probabilistic models of dietary exposure to selected food chemicals. *Food Addit. Contam.* **20**, Suppl. 1, S1–S7.

[21] Glasserman, P., Heidelberger, P., Shahabuddin, P., and Zajic, T. (1999). Multilevel splitting for estimating rare event probabilities. *Oper. Research* **47**, 4, 585–600.

[22] Hall, P. (1997). *The Bootstrap and Edgeworth Expansion*. Springer Series In Statistics. Springer.

[23] IFREMER. (1994-1998). Résultat du réseau national d'observation de la qualité du milieu marin pour les mollusques (RNO).

[24] IPCS. Environmental health criteria 70: Principles for the safety assessment of food additives and contaminants in food. Tech. rep., Geneva, World Health Organisation, International Programme on Chemical Safety. Available from: `www.who.int/pcs/`.

[25] IPCS. (1987). Environmental health criteria 70: Principles for the safety assessment of food. Tech. rep., WHO, Geneva. International Programme on Chemical Safety, available at `www.who.int/pcs/`.

[26] Kella, O. and Stadje, W. (2001). On hitting times for compound Poisson dams with exponential jumps and linear release. *J. Appl. Probab.* **38**, 3, 781–786.

[27] Lagnoux, A. (2006). Rare event simulation. *Probability in the Engineering and Informational Sciences* **20**, 1, 45–66.

[28] MAAPAR. (1998-2002). Résultats des plans de surveillance pour les produits de la mer. Ministère de l'Agriculture, de l'Alimentation, de la Pêche et des Affaires Rurales.

[29] Moral, P. D. (2004). *Feynman-Kac Formulae: Genealogical and Interacting Particle Systems With Applications*. Probability and its applications. Springer, New York.

[30] Rachev, S. and Samorodnitsky, G. (1995). Limit laws for a stochastic process and random recursion arising in probabilistic modelling. *Adv. Appl. Probab.* **27**, 1, 185–202.

[31] Rahola, T., Aaron, R., and Miettienen, J. K. (1972). Half time studies of mercury and cadmium by whole body counting. In *Assessment of Radioactive Contamination in Man*. Proceedings IAEA-SM-150-13, 553–562.

[32] Renwick, A. G., Barlow, S. M., Hertz-Picciotto, I., Boobis, A. R., Dybing, E., Edler, L., Eisenbrand, G., Greig, J. B., Kleiner, J., Lambe, J., Mueller, D., den Brandt, S. T. P. V., Walker, R., and Kroes, R. (2003). Risk characterisation of chemicals in food and diet. *Food Chem. Toxicol.* **41**, 9, 1211–1271.

[33] Rowland, M. and Tozer, T. (1995). *Clinical Pharmacokinetics: Concepts and Applications*.

[34] Smith, J., Allen, P., Turner, M., Most, B., Fisher, H., and Hall, L. (1994). The kinetics of intravenously administered methyl mercury in man. *Toxicol. Appl. Pharmacol. 128*, 251–256.

[35] Smith, J. and Farris, F. (1996). Methyl mercury pharmacokinetics in man: A reevaluation. *Toxicol. Appl. Pharmacol. 137*, 245–252.

[36] Tressou, J. (2005). Méthodes statistiques pour l'évaluation du risque alimentaire. Ph.D. thesis, Université Paris X.

[37] Tressou, J. (2006). Non parametric modelling of the left censorship of analytical data in food risk exposure assessment. *J. Amer. Stat. Assoc.* **101**, 476, 1377–1386.

[38] Tressou, J., Crépet, A., Bertail, P., Feinberg, M. H., and Leblanc, J. C. (2004). Probabilistic exposure assessment to food chemicals based on extreme value theory. application to heavy metals from fish and sea products. *Food Chem. Toxi-*

col. **42**, 8, 1349–1358.
[39] Truhaut, T. (1991). The concept of acceptable daily intake: an historical review. *Food Addit. Contam. 8*, 151–162.
[40] NRC (National Research Council). (2000). Committee on the toxicological effects of methylmercury. Tech. rep., Washington DC.
[41] van der Voet, H., de Mul, A., and van Klaveren, J. D. (2007). A probabilistic model for simultaneous exposure to multiple compounds from food and its use for risk-benefit assessment. *Food Chem. Toxicol.* **45**, 8, 1496–1506.
[42] Verger, P., Tressou, J., and Clémençon, S. (2007). Integration of time as a description parameter in risk characterisation: application to methylmercury. *Regul. Toxicol. Pharmacol.* **49**, 1, 25–30.
[43] Villén-Altamirano, M. and Villén-Altamirano, J. (1991). RESTART: A method for accelerating rare event simulations. In *13th Int. Teletraffic Conference, ITC 13 (Queueing, Performance and Control in ATM)*. Copenhagen, Denmark, 71–76.
[44] Whitt, W. (2002). *Stochastic-Process Limits. An Introduction to Stochastic-Process Limits and their Application to Queues.* Springer.

APPENDIX A: TECHNICAL DETAILS

Though formulated in a fairly abstract manner at first glance, the convergence-preservation results stated in Theorem 1 below are essential from a practical perspective. They automatically ensure, under mild conditions, consistency of simulation-based estimators associated to various functions of statistical interest. Recall that a sequence of estimators $(\hat{F}_n)_{n\in\mathbb{N}}$ of a cumulative distribution function (cdf) F on $\mathbb{R}$ is said to be 'strongly consistent in the L_1-sense' when $M_1(\hat{F}_n, F) = \int_{t\in\mathbb{R}} |\hat{F}_n(t) - F(t)|dt \to 0$ *almost surely*, as $n \to \infty$. Convergence in distribution is denoted by '$\Rightarrow$' in the sequel and we suppose that the Skorohod space $\mathbb{D}_T = \mathbb{D}([0,T])$ is equipped with the Hausdorff metric d_T, the euclidean distance between càd-làg curves (completed with line segments at possible discontinuity points), and with the related $\mathcal{M}_2$ topology.

Theorem 1. (Consistency of simulation estimators, [2]) *Let $0 \leq T \leq \infty$ and for all $n \in \mathbb{N}$, consider a triplet of (random) parameters $(\hat{\theta}_n, \hat{G}_n, \hat{F}_{U,n})$ that almost surely fulfills conditions (i)-(iv) and defines a stochastic exposure process $\hat{X}^{(n)}$. Assume further that $\{(\hat{G}_n, \hat{F}_{U,n})\}_{n\in\mathbb{N}}$ forms an L_1-strongly consistent sequence of estimators of (G, F_U) and that $\hat{\theta}_n$ is a strongly consistent estimator of the pharmacokinetics parameter θ.*

(i) Let $\Psi : (\mathbb{D}_T, d_T) \to \mathbb{R}$ be any measurable function with a set of discontinuity points $Disc(\Psi)$ such that $\mathbb{P}(\{X(t)\}_{t\in(0,T)} \in Disc(\Psi)) = 0$. Then, we almost surely have the convergence in distribution:

$$\Psi(\{\hat{X}^{(n)}(t)\}_{t\in(0,T)}) \Rightarrow \Psi(\{X(t)\}_{t\in(0,T)}), \text{ as } n \to \infty. \tag{17}$$

(ii) Let $\Phi : (\mathbb{D}_T, d_T) \to \mathbb{R}$ be a Lipschitz mapping. Then, the expectations $F(\Phi) = \mathbb{E}[\Phi(\{X(t)\}_{t\in(0,T)})]$ and $\hat{F}_n(\Phi) = \mathbb{E}[\Phi(\{\hat{X}^{(n)}\}_{t\in(0,T)})]$ are both finite. Besides, if $\sup_{n\in\mathbb{N}} \mathbb{E}[\hat{\theta}_n] < \infty$ and $\sup_{n\in\mathbb{N}} \sigma^2_{\hat{G}_n} < \infty$, then the following convergence in mean holds almost surely:

$$\hat{F}_n(\Phi) \to F(\Phi), \text{ as } n \to \infty. \tag{18}$$

Before showing that this result applies to all functionals considered in this paper, a few remarks are in order.

REMARK 5. MONTE-CARLO APPROXIMATION *When $T < \infty$, estimates of the mean $F(\Phi)$ may be obtained in practice by replicating trajectories $\{\hat{X}^{(n),m}\}_{t\in(0,T)}$, $m = 1, \ldots, M$ independently from the distribution parameters $(\hat{\theta}_n, \hat{G}_n, \hat{F}_{U,n})$ and computing the Monte-Carlo approximation to the expectation $\hat{F}_n(\Phi)$, that is*

$$\hat{F}_n^{(M)}(\Phi) = \frac{1}{M} \sum_{m=1}^{M} \Phi(\{\hat{X}^{(n),m}\}_{t\in[0,T]}). \tag{19}$$

REMARK 6. CONDITIONS FULFILLED BY THE DISTRIBUTION ESTIMATES *Practical implementation of the simulation-based estimation procedure proposed above involve computing estimates of the unknown df's, G and F_U, according to a L_1-strongly consistent method. These also have to be instrumental probability distributions on $\mathbb{R}_+$, preferably convenient for simulation by cdf inversion. This may be easily carried out in most situations. In the simple case when the continuous cdf on $\mathbb{R}$, F_{γ_0}, to estimate belongs to some parametric class $\{F_\gamma\}_{\gamma\in\Gamma}$ with parameter set $\Gamma \subset \mathbb{R}^d$ such that $\gamma \mapsto \int |x| dF_\gamma(x)$ and $\gamma \mapsto F_\gamma(t)$ for all $t \geq 0$ are continuous mappings, a natural choice is to consider the cdf $F_{\hat{\gamma}}$ corresponding to a strongly consistent estimator $\hat{\gamma}$ of γ_0 (computed by MLE for instance). In a nonparametric setup, adequate cdf estimators may be obtained using various regularization-based statistical procedures. For instance, under mild hypotheses, the cdf $\hat{F}_n$ associated to a simple histogram density estimator based on an i.i.d. data sample of size n may be shown to classically satisfy, as $n \to \infty$, $\hat{F}_n(x) \to F(x)$ for all x and $\int |x| \hat{F}_n(dx) \to \int |x| F(dx)$ almost surely by straightforward SLLN arguments.*

REMARK 7. RATES OF CONVERGENCE *If the estimator $\hat{G}_n$ converges to G (resp. $\hat{F}_{U,n}$ converges to F_U, resp. $\hat{\theta}_n$ converges to θ) at the rate v_n^G (resp. $v_n^{F_U}$, resp. v_n^θ) in probability as $n \to \infty$, careful examination of Theorem 2's proof in [2] actually shows that convergence (18) takes place in probability at the rate $v_n = \min\{v_n^G,\ v_n^{F_U},\ v_n^\theta\}$.*

For all $T < \infty$, the mapping $x \in \mathbb{D}_T \mapsto \sup_{0 \leq t \leq T} x(t)$ is Lipschitz with respect to the Hausdorff distance, strong consistency of simulation estimators of (10) is thus guaranteed under the assumptions of Theorem 1.

Besides, $\tau_u : x \in \mathbb{D}_\infty \mapsto \inf\{t > 0 : \ x(t) > u\}$ is a continuous mapping in the $\mathcal{M}_2$ topology. Thus, we *almost surely* have $\tau_u(\hat{X}^{(n)}) \Rightarrow \tau_u(X)$ as $n \to \infty$ in the situation of Theorem 1. Furthermore, it may be easily shown that $\{\tau_u(\hat{X}^{(n)})\}_{n \in \mathbb{N}}$ is uniformly integrable under mild additional assumptions, so that convergence in mean also holds *almost surely*.

Similarly, for fixed $T > 0$, the mapping on $(\mathbb{D}_T, d_T)$ that assigns to each trajectory x the temporal mean $T^{-1} \int_{t=0}^{T} x(t)dt$ (respectively, the ratio $T^{-1} \int_{t=0}^{T} \mathbb{I}_{\{x(t) \geq u\}} dt$ of time spent beyond some threshold u) is continuous. Hence, we *almost surely* have the convergence in distribution (respectively, in mean by uniform integrability arguments) of the corresponding simulation estimators as $n \to \infty$.

The next result guarantees consistency for simulation estimators of steady-state parameters, provided that the runlength T increases to infinity at a suitable rate, compared to the accuracy of the instrumental distributions.

THEOREM 2. *(CONSISTENCY FOR STEADY-STATE PARAMETERS, [2]) Let $\phi : \mathbb{R} \to \mathbb{R}$ be any of the three functions $y \mapsto y$, $y \mapsto \mathbb{I}_{\{y \geq u\}}$ or $y \mapsto (y-u)\mathbb{I}_{\{y \geq u\}}$, with $u > 0$. Set $\Phi_T(x) = T^{-1} \int_{t=0}^{T} \phi(x(t))dt$ for any $x \in \mathbb{D}_T$. Assume that Theorem 1's conditions are fulfilled. When $T \to \infty$ and $n \to \infty$ so that both $T^2 \times (M_1(\hat{G}^{(n)}, G) + |\hat{\theta}_n - \theta|)$ and $T \times M_1(\hat{F}_U^{(n)}, F_U)$ almost surely tend to zero, then the following convergences take place almost surely:*

$$\Phi_T(\hat{X}^{(n)}) \Rightarrow \mathcal{L}_\mu(\phi) \text{ and } \hat{F}_n(\Phi_T) \to \mathbb{E}_\mu[\phi(X)], \tag{20}$$

denoting by $\mathcal{L}_\mu(\phi)$ the distribution of $\phi(X)$ when X is drawn from μ.

P. BERTAIL
MODAL'X - UNIVERSITÉ PARIS X
200, AV. DE LA RÉPUBLIQUE
92100 NANTERRE CEDEX, FRANCE
E-MAIL: bertail@ensae.fr

S. CLÉMENÇON
TELECOM PARISTECH
46, RUE BARRAULT
75634 PARIS CEDEX 13, FRANCE
E-MAIL: stephan.clemencon@telecom-paristech.fr

J. TRESSOU
UNITÉ INRA MET@RISK
16, RUE CLAUDE BERNARD
75321 PARIS CEDEX 05, FRANCE
E-MAIL: jessica.tressou@agroparistech.fr